Electrochimica Acta 217 (2016) 24–33

Contents lists available at ScienceDirect

Electrochimica Acta

journal homepage: www.elsevier.com/locate/electacta

Electrochemical Detection of Ultra-trace Cu(II) and Interaction Mechanism Analysis Between Amine-Groups Functionalized $CoFe_2O_4$/Reduced Graphene Oxide Composites and Metal Ion

Shiquan Xiong[a,*], Shoudong Ye[b], Xianhai Hu[c], Fazhi Xie[c]

[a] Key Laboratory of Environmental Toxicology and Pollution Control Technology of Anhui Province, and Key Laboratory of Ion Beam Bioengineering, Hefei Institutes of Physical Science, Chinese Academy of Sciences, Hefei, Anhui 230031, People's Republic of China
[b] School of Life Sciences, Anhui University, Hefei, Anhui 230601, People's Republic of China
[c] School of Materials Science and Chemical Engineering, Anhui Jianzhu University, Hefei 230022, People's Republic of China

ARTICLE INFO

Article history:
Received 21 August 2016
Received in revised form 8 September 2016
Accepted 12 September 2016
Available online 12 September 2016

Keywords:
amine-groups functionalized rGO/$CoFe_2O_4$
copper ion
electroanalysis
interaction mechanism
XPS

ABSTRACT

The polyethylenimine (PEI) or ethanediamine (EDA) has been employed to adsorb metal ions. However, both the combination of $CoFe_2O_4$-reduced graphene oxide (rGO) with PEI or EDA for the analysis of Cu(II) determination and interaction mechanism towards copper ion by electrochemical method and X-ray photoelectron spectroscopy (XPS) are, to the best of our knowledge, unexplored. The amine functionalized rGO/$CoFe_2O_4$ composite were synthesized through a one-pot method, and characterized by electrochemical method and different spectra such as FT-IR, XRD, XPS, etc. The lowest detection limit with 20 pM (3δ method) and sensitivity with 0.39 μA/nM towards Cu(II) was obtained at PEI/rGO/$CoFe_2O_4$ modified electrode under optimized condition. The characteristics of Cu(II) on the amine-group functionalized $CoFe_2O_4$/rGO composite were investigated by cyclic voltammetry and XPS. The shifts of O and N peaks of PEI (or EDA)/$CoFe_2O_4$/rGO preconcentrating Cu(II) showed the synergistic effect of $CoFe_2O_4$/rGO and PEI (or EDA) to Cu(II). The analysis indicated that the interaction between the composite and Cu(II) was adsorption control process. The proposed electrode was also employed to the analysis of real soil sample. Thus, the proposed method and interaction mechanism analysis based on adsorption interaction could provide a reference for further investigate the pollution of metal ions.

1. Introduction

Cu(II), as a common heavy metal ion, is becoming one of the major components of the environmental pollutants, especially in soil, drinking water, etc [1]. The long-term exposure to excess Cu (II) is highly toxic to organisms and the human body [2]. The toxicity of Cu(II) could cause various neurodegenerative diseases such as Menkes, Wilson disease, Alzheimer's and prion diseases, etc [3]. Even intake of small dose could causes nausea, vomiting, diarrhea, hepatic neurosis, gastrointestinal bleeding, hypertension and dermatitis [4]. It is often considered as one of the major hazardous heavy metal ions in the environments, and also on the Environmental Protection Agency's (EPA's) list of priority pollutants [5].

Therefore, the development of accurate and rapid determination method for monitoring Cu(II) in environmental samples is necessary and indispensable. Currently, the usual several approaches have been established for detection of Cu(II) [6–10]. However, the electrochemical method could be recognized as a powerful tool for determination of heavy metal ions (HMI) due to their advantages of simplicity, low cost, good portability, selectivity and high sensitivity [11].

The important question for electrochemical detection of heavy metal ions is the choice of electrode materials. The different nanomaterials or groups modified electrode for determination of copper ion have also been reported in recent years [12–15]. However, the interaction mechanism between materials and metal ions was rarely investigated. M.A. Rahman [16] fabricated a conducting polymer modified electrode by electropolymerization of 3′,4′-diamineterthiophene monomer, the modified electrode showed good affinity to several metal ions such as Cu(II), Co(II), Ni (II), Pb(II) and Hg(II) ions. Heitzmann *et al.* [17] prepared the modified electrode by electropolymerization of N,N'-ethylene bis

* Corresponding author at: 350 Shushanhu Road, Hefei, 230031, Anhui Province, People's Republic of China. Tel.: +86 551 65595670.
E-mail address: xiongshq@mail.ustc.edu.cn (S. Xiong).

http://dx.doi.org/10.1016/j.electacta.2016.09.060
0013-4686/

[N-[(3-(pyrrolelyl)propyl) carbamoyl) methyl]-glycine], which exhibited good performance towards Cu(II), Cd(II) and Pb(II). However, they have no higher selectivity and lower detection limit for the specific metal ions. The surface functionalization methods mostly involved post-synthetic grafting steps, which generally requires expensive organic precursors for grafting, tedious and complicated procedures, longer accumulation time, and harsh experimental conditions. There is a clear unmet need for sensor technologies by functional materials capable of low-cost, simplicity and selective detection of Cu(II) with lower detection limit, and further mechanism research of their interaction.

Among various materials, poly(ethyleneimine) (PEI) is a typical functional macro molecular containing a large quantity of N-donor atoms such as primary, secondary and ternary amine-groups and can combine with different HMI [18,19]. The branched PEI protected silver nanoclusters was successfully synthesized, and acted as sensitive and selective Cu(II) nano-probes for visual Cu(II) monitoring with a 10 nM limit of detection (LOD) [20]. The PEI-based materials for Cu(II) scavenging from ultra-low concentrations in seawater matrixes was reported [21]. The solution of PEI has been used as a novel binding agent of diffusive gradients in thin-films technique for measuring the concentrations of labile Cu (II) [22]. In addition, ethylenediamine-group (EDA) or its composites have also been used to combine with Cu(II) and other HMI. An EDA modified elastomeric network was obtained by the poly condensation reaction, the polymeric networks presented high affinity for the Cu(II) [23]. A novel EDA functionalized chelating resin with high adsorption capacity and significant selectivity for Cu(II) was used in determination Cu(II) from aqueous solutions [24]. Wei produced inorganic–organic hybrid WO*x*-EDA nanowires for adsorption of heavy metal ions [25]. In addition, WO*x*–EDA nanowires with abundant amine-groups was synthesized for selective and sensitive electrochemical determination of HMI [26]. Mwangi reported the performance of the sea weed before and after modification with EDA on adsorption of copper, lead and cadmium ions in aqueous solution [27]. All of these showed that stable complexes between EDA (or PEI) functionalized composites and copper ion could be formed [28]. However, the interaction mechanism between EDA (or PEI) and metal ions was still unclear.

In addition, some iron-based spinel oxides magnetic nanomaterials such as Fe_3O_4 $CoFe_2O_4$, $MnFe_2O_4$, etc have been widely used as an adsorbent for the removal of heavy metal ions from aqueous solution [29–32]. We have reported the determination of several HMI using magnetic Fe_3O_4 and rGO/Fe_3O_4 composites modified electrode [11,33]. So, it tries to perform selective detection of HMI using the Co coped with Fe_3O_4 based on the difference characteristic between Fe_3O_4 and $CoFe_2O_4$. As to our knowledge, $CoFe_2O_4$ was not found to employ to carry out the detection of Cu(II). In addition, $CoFe_2O_4$ suffers from the problems of poor electrical conductivity, graphene sheets has attracted extensive interest in various areas due to their superior electrical conductivity, high surface-to-volume ratio, and ultra-thin thickness properties [34]. To overcome this weakness, the rGO/$CoFe_2O_4$ composites was synthesized by taking rGO as a sense platform to support $CoFe_2O_4$ magnetic particles.

In the case of the reports mentioned above, it is highly desirable to design amine-groups (PEI or EDA) functionalized magnetic composites for selective detection of Cu(II) ions and further analyze the interactive way in detail. In this work, both PEI and EDA were grafted onto the surface of $CoFe_2O_4$/rGO composites, respectively. The synthesized composites modified electrode was applied to carry out the selective detection of Cu(II) under the optimal condition. Based on the adsorption mechanism research between materials and heavy metal ions [35–39], the adsorption mechanism of Cu(II) on amine-groups functionalized $CoFe_2O_4$/rGO composites was analyzed by cyclic voltammetry (CV) and X-ray photoelectron spectroscopy (XPS). The analysis indicated that the process between materials and Cu(II) was surface adsorption, and further confirmed by peaks transfer of N and O elements of XPS. The other interference ions and real sample analysis were also studied. The present study could provide a reference for the study of mechanism between metal ions and materials.

2. Experimental section

2.1. Chemicals and Reagents

Graphite was purchased from Alfa Aesar (Tianjing, China). All of the chemicals (such as anhydrous sodium acetate, $FeCl_3{\cdot}6H_2O$, $CoAc_2{\cdot}6H_2O$ and various metal ions salt, etc) used were of analytical reagent grade from Sinopharm Chemical Reagent Co., Ltd (Shanghai, China) and without further purification. All solutions were prepared with deionized water purified by a Milli-Q purification system (Millipore, USA).

2.2. Instrumentation

Electrochemical experiments were recorded using a CHI 660D computer-controlled electrochemical workstation (CHI Instruments, USA) with a standard three electrode system. A bare glassy carbon electrode (GCE) (diameter of 3 mm) or modified GCE served as a working electrode, a platinum wire was used as a counter-electrode, and a saturated Ag/AgCl electrode as reference electrode. All of electrochemical experiments were carried out in a 10 mL glass cell at room temperature. Square wave anodic stripping voltammetry (SWASV) conditions: frequency, 15 Hz; potential step, 4 mV; pulse amplitude, 25 mV. The differential pulse voltammetry (DPV) method was conducted with a pulse amplitude of 50 mV, pulse width of 50 ms, potential step of 4 mV, and pulse period of 0.2 s. After each measurement, the modified electrode was regenerated in a freshly stirred supporting electrolyte by desorption at 0.5 V for 80 s to remove the target metal from the electrode surface.

The morphologies of nanomaterials were observed by field-emission scanning electron microscopy (SEM) (Quanta 200 FEG, FEI Company, USA). X-ray diffraction (XRD) patterns of the samples were recorded on a Philips X'pert PRO SUPER diffractometer (Netherland) with CuKα radiation. A pH meter (Mettler Toledo FE20, Switzerland) was used for measuring pH. The concentrations of heavy metal ions in soil sample solutions were also determined by an inductively coupled plasma atomic emission spectrophotometer (ICP-AES) (Thermo Fisher Scientic, model ICP 6300). XPS analyses of the samples were conducted using a Thermo ESCALAB 250 spectrometer with an Mg Kα X-ray source (1486.6 eV, 150 W). The structure characteristics of the samples were analyzed using a Fourier-transform infrared (FTIR) spectrometer (Nicolet Co., USA) in the transmission mode, spectra were acquired in the range 400–4000 cm^{-1}. The elemental compositions of the materials were analyzed through energy dispersive X-ray spectroscopy (EDS) (Sirion 200, FEI Co., USA).

2.3. Synthesis of amine-groups functionalized $CoFe_2O_4$/rGO composites

A typical experiment for the synthesis of $CoFe_2O_4$/rGO composites based on the previous reports [33,40] by the addition of $CoAc_2{\cdot}6H_2O$. In brief, 25 mg of GO sheets was dispersed into 40 mL ethylene glycol with sonication for 2 h. Then 0.635 g of $CoAc_2{\cdot}6H_2O$, 3.9 g of NH_4Ac, and 1.35 g of $FeCl_3{\cdot}6H_2O$ were added into the above mixture solution, respectively, and then the mixture solution was stirred for an hour, forming a homogeneous solution

at room temperature. At last, the dispersion solution was transferred into a 50 mL Teflon-lined stainless autoclave, sealed tightly, and heated to 195 °C for 8 h. The product was separated by magnet and washed with ethanol and water for four times, respectively, and then dried in a vacuum oven at 60 °C for 12 h. Thus, the $CoFe_2O_4$/rGO composites were prepared. The synthesized method of amine-groups functionalized $CoFe_2O_4$/rGO composites were similar as that of $CoFe_2O_4$/rGO by addition of 0.4 g of PEI or 25 ml of EDA in reactive mixture.

2.4. The preparation of modified electrodes

The 10 mg of synthesized nanomaterials, such as $CoFe_2O_4$, $CoFe_2O_4$/rGO, PEI(EDA)/$CoFe_2O_4$/rGO, were dispersed in 10 mL of anhydrous alcohol by sonication for 10 min, respectively, and 6 μL aliquot of dispersion were dropped onto the surface of the cleaned GCE, respectively, and dried in air for 4–5 hour at room temperature, forming the modified electrode. Prior to modification, a bare GCE was polished to get a mirror-like surface with 1, 0.3, and 0.05 mm alumina slurry, respectively, rinsed thoroughly with deionized water between each polishing step, then sonicated with 1:1 nitric acid, acetone, and deionized water successively for 3 min, respectively, and dried under a nitrogen atmosphere.

2.5. Preparation of real sample

A soil sample was obtained from Hefei district, accurately weighed (1.0 g) and placed in a ceramic crucible, then transferred into a muffle furnace for ashing at 600 °C for 3 h. Then, the soil sample calcined was placed into conical flask, and treated successively with concentrated HCl, HNO_3, HF and $HClO_4$ solutions in the temperature range of 80 to 230 °C, respectively. Then, the obtained white sample was dried in vacuum, re-diffused into 0.1 M HAc-NaAc buffer solution (pH 6.0) and quantitatively transferred into a 50 mL volumetric flask for further analysis.

3. Results and Discussion

3.1. SEM images and EDS analysis

The typical SEM images of synthesized $CoFe_2O_4$, $CoFe_2O_4$/rGO and PEI/$CoFe_2O_4$/rGO composites are shown in Fig. 1. The diameter of $CoFe_2O_4$ particles is approximately 480 nm as shown in Fig. 1(a), which is the biggest among several particles in Fig. 1. In Fig. 1(b), it can be observed that these $CoFe_2O_4$ particles with sizes of 380 nm are grown on the two-dimensional rGO sheets forming $CoFe_2O_4$/rGO composites, and the average diameter of $CoFe_2O_4$ in PEI/$CoFe_2O_4$/rGO composites is about 220 nm in Fig. 1(c), obviously decreases compared with $CoFe_2O_4$/rGO composites or pure $CoFe_2O_4$ particles, indicating that the synthesis of hydrid composites. In addition, SEM image of EDA/$CoFe_2O_4$/rGO is similar as PEI/$CoFe_2O_4$/rGO (not shown), which could be the reason that the addition of PEI (or EDA) limits the growth of $CoFe_2O_4$ particles based on the previous report [41], the decrease of particle diameter could help improve electron transfer in following electrochemical experiments. It is noted that the amounts of GO added into the

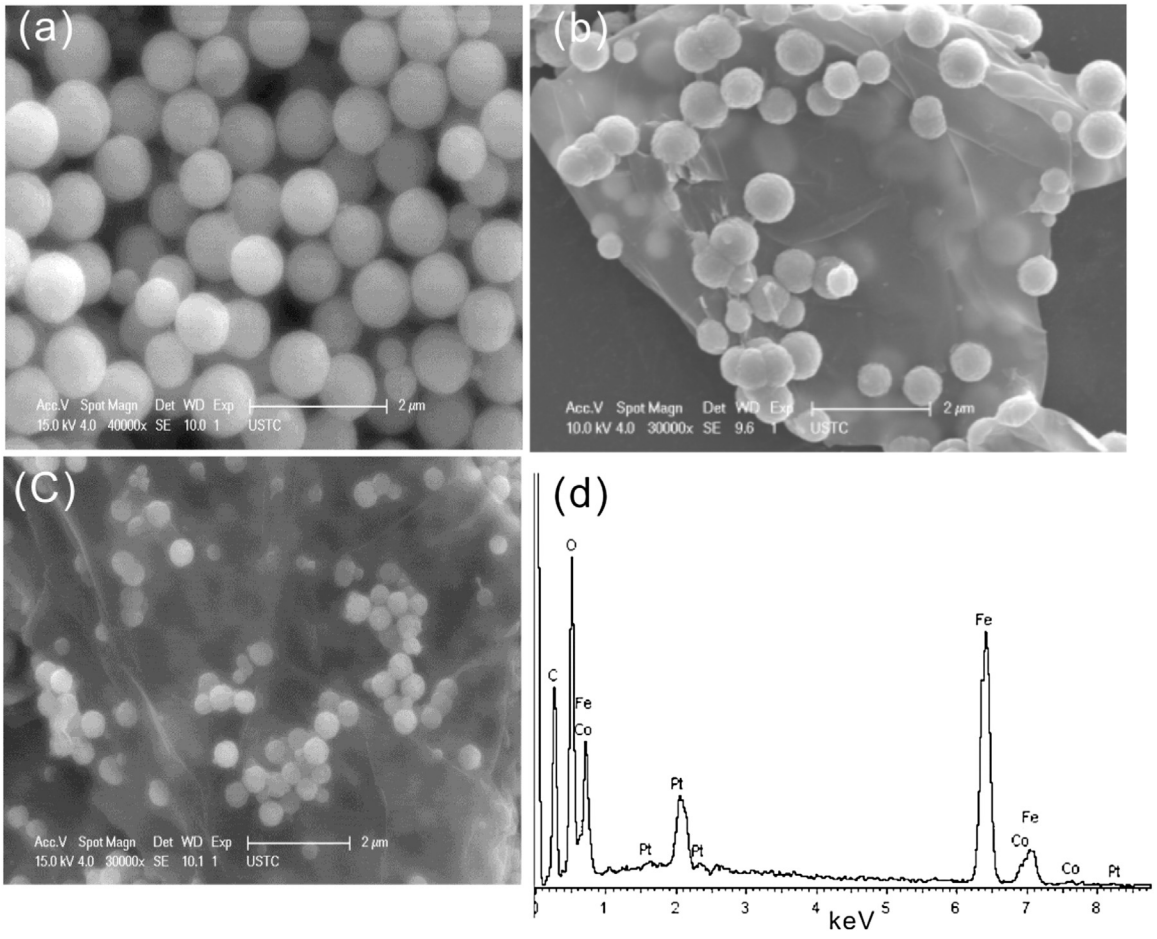

Fig. 1. Typical SEM images of $CoFe_2O_4$ (a), $CoFe_2O_4$/rGO (b), PEI/$CoFe_2O_4$/rGO (c), and EDS of $CoFe_2O_4$/rGO (d).

reactive mixture solution is beyond 25 mg, the morphology characteristics of $CoFe_2O_4$/rGO composites are unchanged, but the sensitivity towards the determination of Cu(II) lowers, thus, 25 mg of GO sheets was chosen for the synthesis of $CoFe_2O_4$/rGO composites. In addition, the amounts of PEI (or EDA) added into the reactive mixture solution is beyond 0.4 g (or 25 mL EDA), and the detectable lowest concentration for Cu(II) lowers in the following experiments, hence, 0.4 g of PEI (or 25 mL of EDA) was chosen for the synthesis of PEI (or EDA)/$CoFe_2O_4$/rGO compsites. In addition, EDS is also used to analyze the chemical composition, the result is shown in Fig. 2(d), there are four different elements, such as Fe, Co, C, and O, present on the hybrid surface, indicating the preparation of rGO/$CoFe_2O_4$ composites.

3.2. XRD patterns and FT-IR spectra analysis

XRD experiments of materials are performed to identify the crystallographic structure different $CoFe_2O_4$ particles. The major crystal phase of pure $CoFe_2O_4$ is in a good agreement with JCPDS: 22/1086 in Fig. 2(A-a). As can be observed that $CoFe_2O_4$/rGO exhibit the typical pattern of spinel ferrite with seven well-defined peaks occurring at $2\theta = 18.32^\circ$, 30.20°, 35.56°, 43.10°, 53.48°, 56.98°, and 62.56° in Fig. 2(A-b). These peaks correspond to the Bragg planes of (111), (222), (311), (400), (422), (511), and (440) in accordance with $CoFe_2O_4$ particles [30]. The positions of diffraction peaks indicate that the $CoFe_2O_4$/rGO composites are prepared [42]. From Fig. 2(A-c), the XRD patterns of PEI (or EDA)/$CoFe_2O_4$/rGO composites are also similar as that of $CoFe_2O_4$/rGO composites, implying that the crystal $CoFe_2O_4$ remains the same even during the solvothermal reaction with the addition of PEI (or EDA). However, the peaks of XRD become wider and reduced with the addition of PEI (or EDA) in Fig. 2 (A-c, d), indicating the sizes of crystallic particles decreased, in accordance with the SEM images in Fig. 1.

FTIR spectra of EDA/$CoFe_2O_4$/rGO and PEI/$CoFe_2O_4$/rGO are shown in Fig. 2(B). The characteristic peak appears at 1034 cm^{-1} corresponds to C–O stretching vibrations in $CoFe_2O_4$/rGO, respectively [43]. The strong absorption peak at 530 cm^{-1} are due to the intrinsic stretching vibrations of metal oxygen bands at tetrahedral sub-lattices confirming the formation of $CoFe_2O_4$ in Fig. 2(B–a, b) [44]. Bands around 1,660 and 1670 cm^{-1} correspond to N–H bending vibration in PEI/$CoFe_2O_4$/rGO and EDA/$CoFe_2O_4$/rGO composites in Fig. 2(B–c,d), it is $—NH_2$ rather than protonated $—NH_3^+$, lack a characteristic peak located at 2100 cm^{-1}, indicating the synthesis of amine-groups functionalized $CoFe_2O_4$/rGO composites [45–47]. The intense band at 3,500 cm^{-1} indicates the stretching vibration of O–H in H_2O molecular.

3.3. XPS analysis of the composites

To further understand the chemical compositions and oxidation states of PEI (or EDA)/$CoFe_2O_4$/rGO composites, XPS measurements are performed in the range of 0 to 1100 eV, the corresponding results are shown in Fig. 3(a–d). The survey spectrum indicates the presence of the elements Co, Fe, O, N and C in Fig. 3(a). The peak locates at 284.8 eV is assigned to the characteristic peak of C 1 s in Fig. 3(a), indicating the presense of reduced graphene oxide. The peak at about 400 eV in the N 1 s spectrum is assigned to the nitrogen element in association with PEI. The high-resolution N 1 s spectrum reveals the presence of amide (398.5 eV), amine-group (399.9 eV) due to the formation of O—N and C—N in the hydrid materials, respectively, rather than that of alkylammonium (402.4 eV) [48,49]. This indicates that the PEI molecules is intercalated in the composites. The two characteristic peaks with binding energies of around 781.6 and 787.2 eV in Fig. 3(c) are ascribed to Co $2p_{3/2}$ and its shake-up satellites, respectively. The other two peaks around 797.7 and 803.8 eV are Co $2p_{1/2}$ and its shake-up satellite, respectively, confirming the chemical state as Co(II). Fig. 3(d) shows the high-resolution Fe 2p spectrum, two peaks at 724.8 and 711.5 eV corresponds to Fe $2p_{3/2}$ and Fe $2p_{1/2}$ of $CoFe_2O_4$, respectively, confirming the chemical state as Fe(III) [30,50]. The proportions of C, N, Fe, Co and O elements in PEI/$CoFe_2O_4$/rGO composites are 38.2, 7.05, 13.11, 5.8 and 35.85%, rather than the proportion of the mixture including PEI, $CoFe_2O_4$ and rGO added into autoclave. XPS measurement results outlined above support the result of XRD, indicating that the preparation of amine-group functionlized $FeCo_2O_4$/rGO hybrid composites [48].

3.4. Electrochemical characteristics of different modified electrodes

The electrochemical characteristics of $CoFe_2O_4$, rGO, $CoFe_2O_4$/rGO, EDA/$CoFe_2O_4$/rGO and PEI/$CoFe_2O_4$/rGO modified electrodes are analyzed by CV and electrochemical impedance spectroscopy in 5 mM $Fe(CN)_6^{3-}$ solution (Fig. S1, Supporting Information), which show that the electrochemical characteristics and relationship between current difference and the impedance values of different electrodes. And the electrochemical active areas for $CoFe_2O_4$, rGO, $CoFe_2O_4$/rGO, EDA/$CoFe_2O_4$/rGO and PEI/$CoFe_2O_4$/rGO are calculated to be 0.076, 0.087, 0.084, 0.091 and 0.125 cm^2 by the Randles-Sevcik equation, $I_{pc} = 2.69 \times 10^5 n^{3/2} A C D^{1/2} v^{1/2}$, respectively, where I_{pc} is the reduction peak current, n is the electron transfer number, A is the apparent electrode area (cm^2), D is the diffusion coefficient of $K_3[Fe(CN)_6]$ ($cm^2\ s^{-1}$), C is the concentration of $K_3[Fe(CN)_6]$ (mol L^{-1}) and v is the scan rate (V s^{-1}). It can be seen that the active area of PEI/$CoFe_2O_4$/rGO electrode is the largest in the several modified electrodes mentioned above. And the

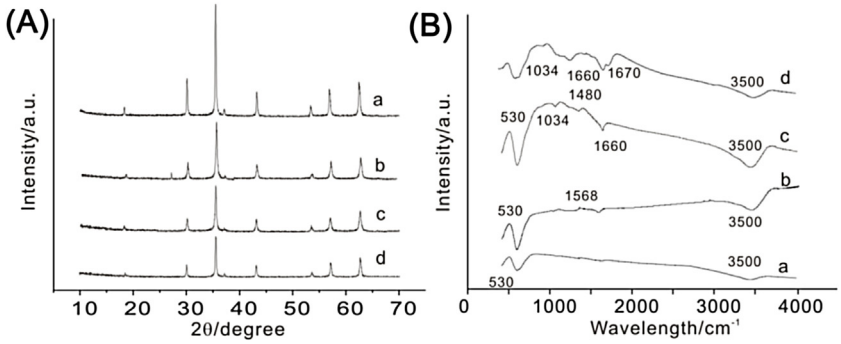

Fig. 2. (A) XRD patterns of $CoFe_2O_4$ (a), $CoFe_2O_4$/rGO (b), EDA/$CoFe_2O_4$/rGO (c), PEI/$CoFe_2O_4$/rGO (d). (B) FTIR spectra of $CoFe_2O_4$ (a), $CoFe_2O_4$/rGO (b), EDA/$CoFe_2O_4$/rGO (c), PEI/$CoFe_2O_4$/rGO (d).

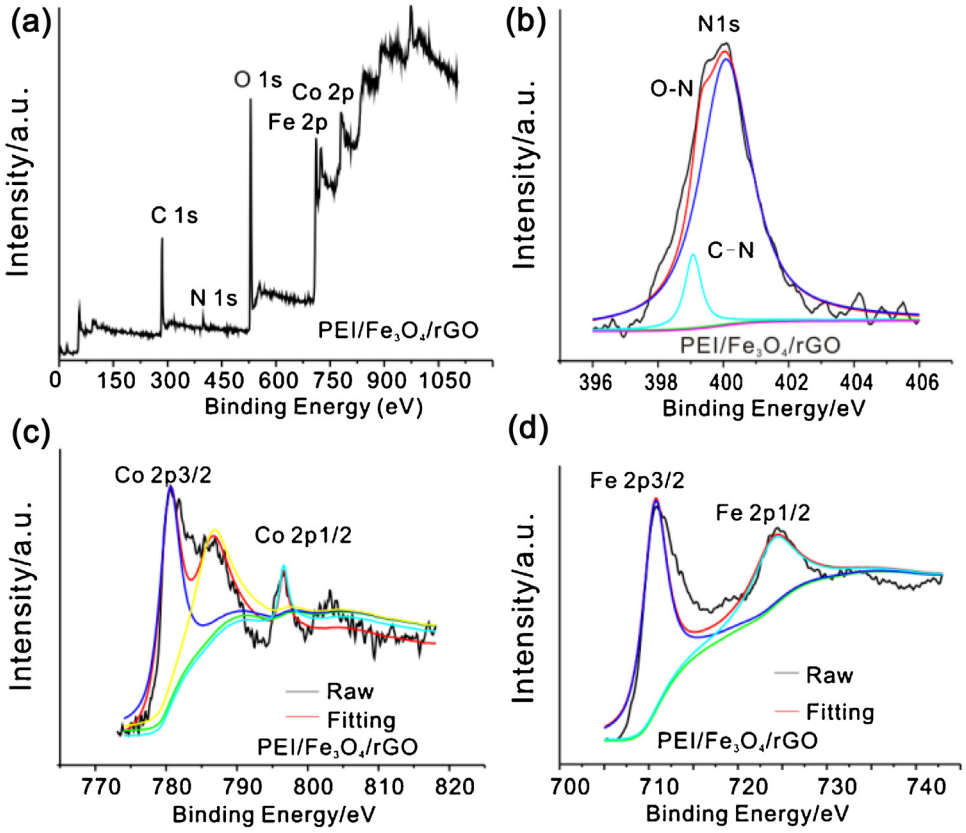

Fig. 3. XPS spectra analysis of PEI/$CoFe_2O_4$/rGO composites. (a) Survey spectrum of PEI/$CoFe_2O_4$/rGO composites, high resolution N (b), Co (c) and Fe (d) spectra of PEI/$CoFe_2O_4$/rGO composites.

experimental results shows that the detection effect of PEI/$CoFe_2O_4$/rGO electrode towards Cu(II) is the best in the detection limit and sensitivity.

3.5. Electrochemical responses of the modified electrodes towards Cu (II)

The $CoFe_2O_4$, $CoFe_2O_4$/rGO, EDA/$CoFe_2O_4$/rGO, PEI/$CoFe_2O_4$/rGO modified GCEs are applied to perform the analysis of Cu(II) containing 0.1 μM solution by SWASV, respectively, and these analytical performances are shown in Fig. 4(a). No peak is found at $CoFe_2O_4$ modified electrode, there is a small stripping peak appearing at potentials of −0.05 V towards $CoFe_2O_4$/rGO electrode, a high stripping current appeared at EDA/$CoFe_2O_4$/rGO modified electrode, and the biggest stripping current is observed at PEI/$CoFe_2O_4$/rGO electrode, indicating that PEI/$CoFe_2O_4$/rGO electrode has the best response towards Cu(II).

3.6. The response of Cu(II) using different electrochemical methods

To further examine the voltammetric performance of PEI/$CoFe_2O_4$/rGO composite modified electrode. The comparison of CV, DPV, and SWASV of 3 μM Cu(II) response on PEI/$CoFe_2O_4$/rGO composite modified GCE is shown in Fig. 4(b). In cyclic voltammogram, a reduction wave emerged at −0.13 V (vs Ag/AgCl), which is attributed to one-electron reduction of Cu(II) to Cu(I), on the reversal anodic scan, an oxidation wave at 0.08 V is observed. This process is ascribed to the subsequent re-oxidation of Cu(I) to Cu(II) species [51–53]. The anodic peak current for DPV is observed in Fig. 4(b) and larger than that of CV. SWASV of PEI/Fe_3O_4/rGO composite modified electrode reveals a distinctive anodic peak at 0.2 V associated with oxidization of Cu(I)/Cu(II), it can be observed that the anodic stripping current of SWASV is the largest among three electrochemical techniques, the anodic current using CV is the least, thus, the maximum response is obtained through SWASV.

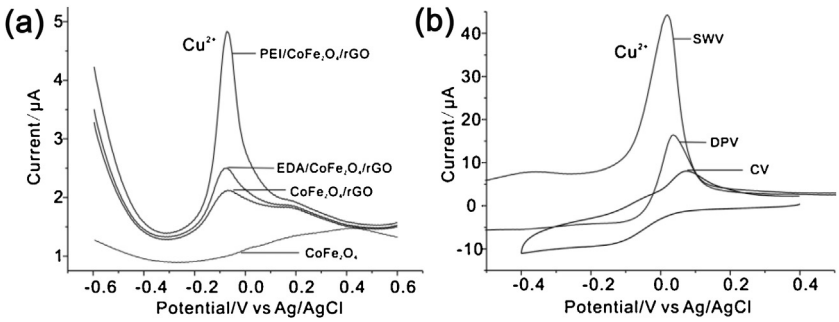

Fig. 4. The typical stripping responses of the $CoFe_2O_4$, rGO/$CoFe_2O_4$, EDA/rGO/$CoFe_2O_4$, PEI/rGO/$CoFe_2O_4$ modified electrodes in 0.1 M NaAc-HAc solution (pH 6.0) containing 0.1 μM Cu(II) (a). The SWASV, DPV and CV responses of 3 μM Cu(II) at PEI/rGO/$CoFe_2O_4$ modified electrode (b).

Thus, SWASV is selected to carry out the detection of Cu(II) in the following experiment. In addition, the stripping potential obtained using SWASV is the least compared with those of CV and DPV, indicating that the stripping of Cu is finished easily by SWASV. Thus, the SWASV is employed to carry out the detection of Cu(II) in the following experiments.

3.7. Electrochemical measurments of Cu(II) by SWASV.

To further and systematically investigate the stripping performance of copper, SWASV is employed to perform the detemination of Cu(II), at first, Cu is deposited on the surface of electrode by negative potential, Cu(II) ion is stripped by a successive potential, then stripping peak currents in different concentrations can be recorded. The four kinds of modified electrodes, such as $CoFe_2O_4$, $CoFe_2O_4$/rGO, EDA/$CoFe_2O_4$/rGO, PEI/$CoFe_2O_4$/rGO are carried out the determination of Cu(II) according to the optimal conditions (Fig. S2), respectively. It can be observed that the peak currents of Cu increase with the increasing concentrations at different modified electrodes in Fig. 5(a–d). The insets are the calibration curves of Cu(II) concentrations towards stripping currents, respectively.

As can be seen in Fig. 5(a), the currents for $CoFe_2O_4$ electrode linearly increase with the successive addition of standard solution of Cu(II) in a concentration range from 200 to 1600 nM, the linear regression equation is I (μA) = −3.45 + 0.011C (nM), with correlation coefficient of 0.993, the detection limit calculated is 58 nM, the sensitivity is 0.011 μA/nM, and the lowest detectable concentration is 200 nM. As shown in Fig. 5(b), the linear equation for $CoFe_2O_4$/rGO modified electrode is I (μA) = −1.95 + 0.027C (nM) in the concentration range from 50 to 1350 nM, the sensitivity is 0.027 μA/nM, which is about 3-fold of that for $CoFe_2O_4$ electrode. The LOD of 18 nM was obtained, three times less than that of $CoFe_2O_4$ electrode. In addition, the stripping potential (−0.05 V) for $CoFe_2O_4$/rGO modified electrode is less than that (−0.08 V) of $CoFe_2O_4$ modified electrode due to the catalysis of good conductivity of graphene.

As for amine-groups functionalized $CoFe_2O_4$/rGO modified GCEs shown in Fig. 5(c, d), the linear equation for EDA/$CoFe_2O_4$/rGO/GCE is I (μA) = 0.14 + 0.0145C (nM) in a concentration range from 8 to 250 nM, with the correlation coefficient of 0.992, the sensitivity is 0.0145 μA/nM, the corresponding LOD calculated is 2 nM. As for PEI/$CoFe_2O_4$/rGO/GCE, the detection of Cu(II) was performed in the range of 0.5 to 10 nM, and the corresponding linear equation: I (μA) = 0.06 + 0.39C (nM) with the detection limit of 0.02 nM, the sensitivity is 0.39 μA/nM and more than twenty seven times that of EDA/$CoFe_2O_4$/rGO. The LOD of PEI/$CoFe_2O_4$/rGO/GCE towards determination of Cu(II) with 0.02 nM is the lowest among four kinds of modified electrodes, and about one thousand four hundred and fifty, four hundred and fifty, and fifty times less than those of $CoFe_2O_4$, $CoFe_2O_4$/rGO, EDA/$CoFe_2O_4$/rGO modified electrodes. The higher sensitivity and lowest detection limit might be attributed to synergistic interaction between rGO/$CoFe_2O_4$ and PEI to Cu(II), the high surface area and porous morphology of rGO/$CoFe_2O_4$ with PEI could cause strong physical absorption, and a lot of amine-groups of PEI can even chelate ultra amount of copper ions. In addition, the mixture, including PEI, $CoFe_2O_4$ and GO according to the above proportion of synthesized composites, modified electrode is also employed to perform the determination of Cu(II), and the determination results are shown in Fig. S3. The results indicate that the sensitivity for mixture modified electrode is obviously lower, and the detection limit is also higher in comparison with PEI/$CoFe_2O_4$/rGO electrode.

All of the same modified electrodes are repeated three times with good reproducibility as the obtained relative standard

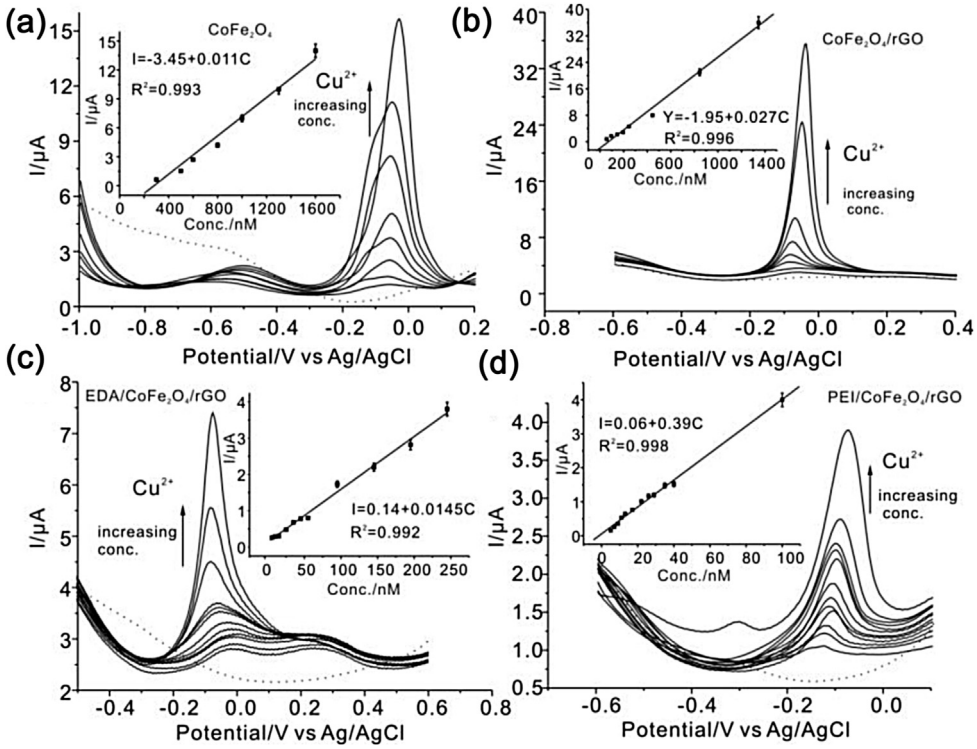

Fig. 5. Typical SWASV responses of $CoFe_2O_4$ (a), $CoFe_2O_4$/rGO (b), EDA/$CoFe_2O_4$/rGO (c) and PEI/$CoFe_2O_4$/rGO (d) modified electrodes for the analysis of Cu(II) containing different concentrations in 0.1 M NaAc-HAc solution (pH 6.0), dotted lines refer to the base lines. Insets in panels (a–d) are the corresponding linear calibration plots of peak current towards Cu(II) concentrations, respectively.

Table 1
Comparison of performance of the PEI/$CoFe_2O_4$/rGO/GCE and other electrodes for Cu(II) detection.

Electrode materials	LOD (nM)	Sensitivity (μA/μM)	Detection range (μM)	References
TPAASH	80	–	0.6–11	[15]
EDTA-CPME	0.2	0.575	0.001–0.1	[16]
PPy array	46	–	0.1–30	[55]
MOFs	11	0.58	1–10	[56]
Hg-based SPE	4	3.23	–	[17]
MWCNTs/CHIT/SPE	12	0.45	0.04–0.2	[57]
AuNPs	–	4.18	0.3–1.4	[58]
PEI/$CoFe_2O_4$/rGO	0. 4	39	0.003– 0.1	This method

2,2′,2″-(2,2′,2″-nitrilotris(ethane-2,1-diyl)-tris((pyridin-2-ylmethyl)azanediyl)triethanethiol (TPAASH), polymerization of 3′,4′-diamine-2,2′;5′,2″-terthiophene (EDTA-CPME), Polypyrrole (PPy), Carbon paste electrode (CPE), metal-organic frameworks (MOFs), screen printed electrode (SPE), chitosan (CHIT), nanoparticles (NPs), multi-walled carbon nanotubes (MWCNTs).

deviations (RSDs) are all less than 3.5%, showing good repeatability of the modified electrodes.

3.8. Comparison with other electrochemical methods

To understand the effect of PEI/$CoFe_2O_4$/rGO/GCE, a detailed comparison with those reported previously is summarized in Table 1. It can be seen that the PEI/$CoFe_2O_4$/rGO has a lower detection limit and higher sensitivity toward Cu(II) than most others electrodes for the determination of Cu(II). The excellent sensitivity of the sensor benefits from the improvement on graphene, in addition, the contact surface area of porous $CoFe_2O$ toward Cu(II) become larger, increasing the reactive-sites of PEI, and lowering the LOD of Cu(II).

3.9. Interference studies

The interference studies of the PEI/$CoFe_2O_4$/rGO electrode toward Cu(II) are evaluated by testing the SWASV behaviors in presence of Cu(II) solution (100 nM) containing other ions such as Cr(II), Pb(II), Ni(II), Zn(II), Gd(II), Mg(II), Cd(II), Ca(II), K(I), Na(I), Fe (II), Fe(III) and Hg(II) at 10 μM, which might coexist in the polluted environment systems, are chosen as interfering ions for investigating the selectivity of PEI/$CoFe_2O_4$/rGO modified electrode. As shown in Fig. 6, the results indicate that little current signal could be observed for each metal ion mentioned above. It is clear that the obtained stripping current toward Cu(II) including 100 nM is around 30–50 times higher than others in presence of 10 μM, indicating that PEI/$CoFe_2O_4$/rGO modified electrode has good selectivity for the detection of Cu(II), which is attributed to the selective transportation of Cu(II) from the sample solution to the electrode surface via the stronger affinity of PEI/$CoFe_2O_4$/rGO composites.

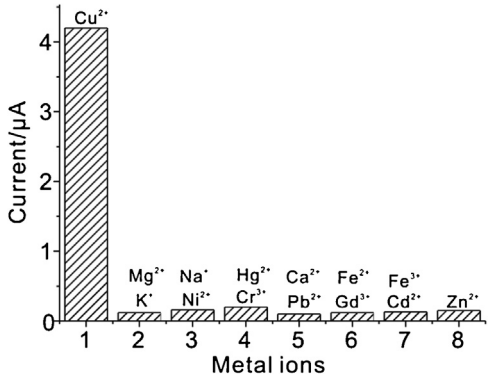

Fig. 6. Interference experiments of Cu(II) containing different metal ions.

3.10. Characterization of Cu(II) on amine-groups functionlized $CoFe_2O_4$/rGO composites

To understand the interactive characteristics between Cu(II) and amine-groups functionlized $CoFe_2O_4$/rGO composites, CV is first used to investigate the reduction process of Cu(II) at the PEI/$CoFe_2O_4$/rGO modified GCE. Fig. 7(a) shows the recorded cyclic voltammograms of 10 μM Cu(II) on PEI/$CoFe_2O_4$/rGO electrode at different scan rates (0.02–0.08 V s^{-1}) in 0.1 M acetate buffer (pH 6). The reduction peak appears at −0.16 V, then the potential of peak slowly shifts to −0.21 V with the increasing scan rate. It can be seen that the reduction peak current increase with the scan rate increasing. The reduction peak potential shifts towards more positive values with increasing scan rate, which is typical features of the irreversible electrochemical reaction [54]. It is found that the reduction peak current is proportional to the potential scan rate in Fig. 7(b), the regression equation for the relationship is: I (μA) = 57.75 v (V s^{-1}) + 6.38 (R^2 = 0.995), indicating the reduction reaction of Cu(II) is a surface-reaction-controlled process, instead of a diffusion-controlled process. At similar condition, the relationship plot between the reduction peak current and scan rate (v) at EDA/$CoFe_2O_4$/rGO modified GCE is observed in Fig. S4, indicating that it is also a surface-controlled process. It shows that Cu(II) had stronger absorption on the amine-groups functionalized $CoFe_2O_4$/rGO surface.

To further show the characteristic of Cu(II) on a PEI/$CoFe_2O_4$/rGO composite surface, XPS experiments is performed. Both PEI/$CoFe_2O_4$/rGO and EDA/$CoFe_2O_4$/rGO composites modified electrodes are dipped in the solution of 30 μM Cu(II) with stirring for the adsorption, respectively. Two similar reduction peak of Cu(II) are observed (the figures not shown). The voltammetric experiments indicate that Cu(II) have strong adsorption on the PEI (or EDA)/$CoFe_2O_4$/rGO surface. At the same time, the typical XPS spectra PEI/$CoFe_2O_4$/rGO composites with Cu(II) is shown in Fig. 8. It displays the survey spectrum of EDA/$CoFe_2O_4$/rGO absorbed by Cu (II). The fitting peaks at around 934.5 and 954.6 eV for Cu(II) $2p_{3/2}$ and $2p_{1/2}$ peaks demonstrate that the chemical valence of Cu at the surface of the EDA/$CoFe_2O_4$/rGO composites is a valence states of +2 in Fig. 8(b), indicating Cu(II) is adsorbed on the surface of composites [48].

The peaks of the O 1s and the N 1s with satellite (401.8 eV) have shifts of 0.4 and 0.2 eV to higher binding energies for PEI/$CoFe_2O_4$/rGO after preconcentrating Cu(II) in Fig. 9(c,d), respectively, indicating that interactions occurred between PEI/$CoFe_2O_4$/rGO and Cu(II) in Fig. 8(c,d), which is the synergistic effect of amine-groups of PEI and OH group of $CoFe_2O_4$ towards Cu(II).

The XPS of EDA/$CoFe_2O_4$/rGO composites is also similar as that of PEI/$CoFe_2O_4$/rGO. The inset of Fig. 8(d) shows the intensity of Cu 2p on PEI/$CoFe_2O_4$/rGO composites increases compared with that of EDA/$CoFe_2O_4$/rGO under preconcentrating the same Cu(II) concentration (and the corresponding stripping current mentioned above on EDA/$CoFe_2O_4$/rGO electrode is also larger than that

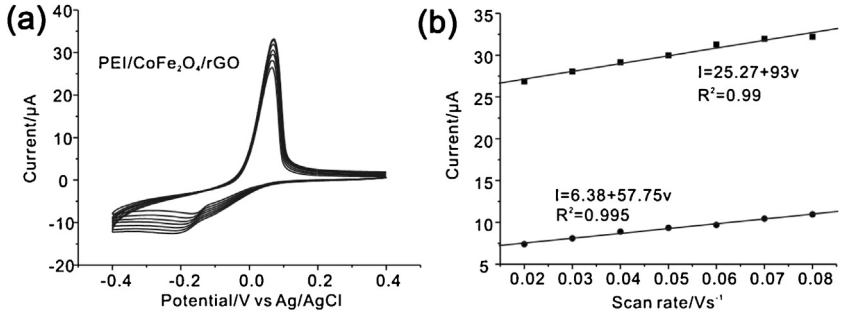

Fig. 7. Cyclic voltammograms of the PEI/$CoFe_2O_4$/rGO modified GCE with different potential scan rate (0.02–0.08 V s^{-1}) in acetate buffer (pH 6) containing 10 μM Cu(II). Inset is the relationship plot between the reduction peak current of Cu(II) and scan rate.

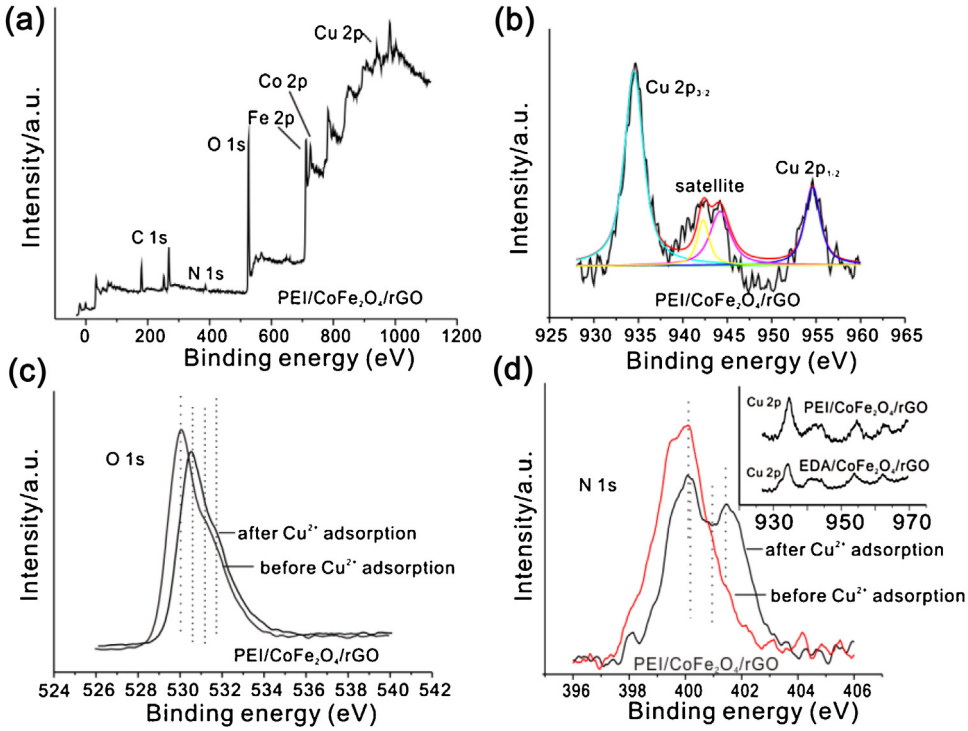

Fig. 8. XPS spectra of PEI/$CoFe_2O_4$/rGO composites: (a) survey spectrum of PEI/$CoFe_2O_4$/rGO composites after adsorbing Cu(II), (b) high resolution Cu 2p spectrum on the surface of PEI/$CoFe_2O_4$/rGO composites after adsorbing Cu(II), (c) high resolution spectrum of O 1s on the surface of PEI/$CoFe_2O_4$/rGO composites after and before adsorbing Cu(II), (d) high resolution spectrum of N 1s on the surface of PEI/$CoFe_2O_4$/rGO composites after and before adsorbing Cu(II), inset is Cu 2p spectra intensity comparison of PEI/$CoFe_2O_4$/rGO and EDA/$CoFe_2O_4$/rGO composites after preconcentrating Cu(II).

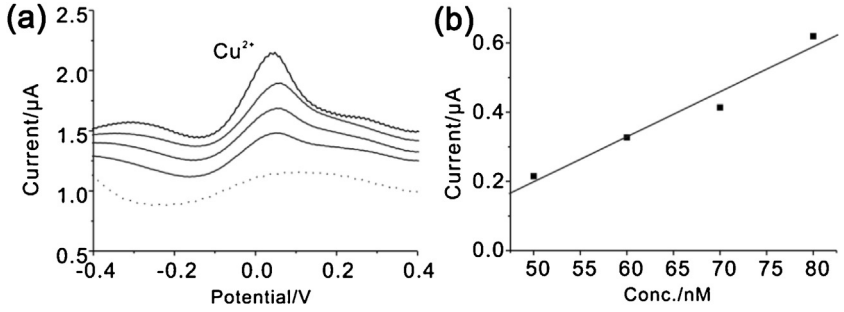

Fig. 9. SWASV responses of PEI/$CoFe_2O_4$/rGO modified GCE toward Cu(II) in a soil sample solution by standard addition method in 0.1 M NaAc-HAc solution (pH 6.0) (a). The relationship between peak currents and concentrations of Cu(II) (b). The dotted line refers to the SWASV response in the absence of Cu(II).

Table 2
Standard deviations of AES and present method for the detection of Cu(II).

Methods	1	2	3	4	5	6	SD (%)
AES (μg/kg)	10	8	9	9	12	6	3.67
PM (μg/kg)	8	9	12	7	11	7	2.16

PM: Present method, AES: atom emission spectrum, SD: standard deviation 1-6: Times of detection.

of EDA/$CoFe_2O_4$/rGO), indicating more amounts of Cu(II) is preconcentrated on the surface of PEI/$CoFe_2O_4$/rGO. The XPS spectra are consistent with our electrochemical results above mentioned. And the results prove the presence of metal Cu(II) is absorbed on the surface of composites.

3.11. Analysis of real samples

In order to evaluate the application performance of the sensor, the determination of Cu(II) in real sample is performed using the standard addition method. Three real soil are collected and treated. The PEI/$CoFe_2O_4$/rGO nanocomposite modified electrode is used directly to determine the Cu(II) treated soil solution first. Then, the solutions of analytical soil samples are spiked with Cu (II) at different concentration levels, and then analyzed with the proposed electrode. As shown in Fig. 9(a, b), the original Cu(II) concentration in the soil sample is tested to be 15 μg/kg, which is far lower than the standard of USA and UC. The accuracy of the method is also assessed by comparing the results of electrochemical detection with those obtained by ICP-AES in Table 2. The results indicate that the proposed method is highly accurate, which can be used for direct analysis of real soil samples. The experiments are repeated six times with good reproducibility as the obtained relative standard deviations (RSDs) are all less than 4%.

4. Conclusions

The amine-groups functionalized $CoFe_2O_4$/rGO composite are prepared, characterized and applied for the detection of metal ion. Especially, the PEI/$CoFe_2O_4$/rGO composites modified electrode exhibits the lowest detection limit, good selectivity and the highest sensitivity towards Cu(II) at ultra-trace levels compared with others. The interactive mechanism between amine-groups functionalized $CoFe_2O_4$/rGO composites and Cu(II) is investigated by CV and XPS, indicating that adsorption process could be primary. The excellent electrochemical properties of amine-groups $CoFe_2O_4$/rGO electrode might be ascribed to the special porous morphology of $CoFe_2O_4$/rGO, as well as the good chelating ability of PEI. The electrochemical sensor could be also employed to determine Cu(II) in real samples with satisfactory results. It is expected that the research of interactive mechanism between amine-groups functionalized porous magnetic materials and copper ions could offer a potential application for analysis and detection of metal ions.

Acknowledgements

The authors acknowledge financial support from HIPS (Y49LH55893), CAS.

Appendix A. Supplementary data

Supplementary data associated with this article can be found, in the online version, at http://dx.doi.org/10.1016/j.electacta.2016.09.060.

References

[1] Z.Y. Yao, Y.B. Yang, X.L. Chen, X.P. Hu, L. Zhang, L. Liu, Y.L. Zhao, H.C. Wu, Visual detection of copper (II) ions based on an anionic polythiophene derivative using click chemistry, Anal. Chem. 85 (2013) 5650–5653.
[2] Y. Zhou, S.X. Wang, K. Zhang, X.Y. Jiang, Visual detection of copper (II) by azide- and alkyne-functionalized gold nanoparticles using click chemistry, Angew. Chem. Int. Ed. 120 (2008) 7564–7566.
[3] Y.J. Song, K.G. Qu, C. Xu, J.S. Ren, X.G. Qu, Visual and quantitative detection of copper ions using magnetic silica nanoparticles clicked on multi-walled carbon nanotube, Chem. Commun. 46 (2010) 6572–6574.
[4] H. Karen, A. Verónica, R.R. Carlos, Levels of copper in sweeteners, sugar, tea, coffee and mate infusions. Determination by adsorptive stripping voltammetry in the presence of α/lipoic acid, Microchem. J. 119 (2015) 11–16.
[5] Z. Szigeti, I. Bitter, K. Toth, C. Latkoczy, D.J. Fliegel, D. Gunther, E. Pretsch, A novel polymeric membrane electrode for the potentiometric analysis of Cu^{2+} in drinking water, Anal. Chim. Acta 532 (2005) 129–136.
[6] C.A. Sahin, I. Tokgöz, A novel solidified floating organic drop microextraction method for preconcentration and determination of copper ions by flow injection flame atomic absorption spectrometry, Anal. Chim. Acta 667 (2010) 83–87.
[7] M.S. Chan, S.D. Huang, Direct determination of cadmium and copper in seawater using a transversely heated graphite furnace atomic absorption spectrometer with Zeeman-effect background corrector, Talanta 51 (2000) 373–380.
[8] F.T. Lv, X.L. Feng, H.W. Tang, L.B. Liu, Q. Yang, S. Wang, Development of film sensors based on conjugated polymers for copper(II) ion detection, Adv. Funct. Mater. 21 (2011) 845–850.
[9] A. Blazewicz, W. Dolliver, S. Sivsammye, A. Deol, R. Randhawa, G. Orlicz-Szczesna, R. Blazewicz, Determination of cadmium, cobalt, copper, iron, manganese, and zinc in thyroid glands of patients with diagnosed nodular goitre using ion chromatography, J. Chromatogr. B 878 (2010) 34–38.
[10] M.C. Ana, J. Angeles, C. Ana, G. Fernando, I.L. Alejandro, S. Enrique, M.C. Ana, Development and validation of an inductively coupled plasma mass spectrometry (ICP-MS) method for the determination of cobalt, chromium, copper and nickel in oral mucosa cells, Microchem. J. 114 (2014) 73–79.
[11] S.Q. Xiong, M. Wang, D.Q. Cai, Y. Li, N.Y. Gu, Z.Y. Wu, Electrochemical detection of Pb(II) by glassy carbon electrode modified with amine-group/functionalized magnetite nanoparticles, Anal. Lett. 46 (2013) 912–922.
[12] S. Chaiyo, O. Chailapakul, T. Sakai, N. Teshima, W. Siangproh, Highly sensitive determination of trace copper in food by adsorptive stripping voltammetry in the presence of 1 10-phenanthroline, Talanta 108 (2013) 1–6.
[13] S. Abbasi, H. Khani, R. Tabaraki, Highly sensitive determination of trace copper in food by adsorptive stripping voltammetry in the presence of 1 10-phenanthroline, Food Chem. 123 (2010) 507–512.
[14] Y. Liao, Q. Li, Y. Yue, S.J. Shao, Selective electrochemical determination of trace level copper using a salicylaldehyde azine/MWCNTs/Nafion modified pyrolytic graphite electrode by the anodic stripping voltammetric method, RSC Adv. 5 (2015) 3232–3238.
[15] L.M. Zhang, Y.Y. Han, F. Zhao, G.Y. Shi, Y. Tian, A selective and accurate ratiometric electrochemical biosensor for monitoring of Cu^{2+} ions in a rat brain, Anal. Chem. 87 (2015) 2931–2936.
[16] M.A. Rahman, M.S. Won, Y.B. Shim, Characterization of an EDTA bonded conducting polymer modified electrode: its application for the simultaneous determination of heavy metal ions, Anal. Chem. 75 (2003) 1123–1129.
[17] M. Heitzmann, C. Bucher, J.C. Moutet, E. Pereira, B.L. Rivas, G. Royal, E. Saint Aman, Complexation of poly(pyrrole-EDTA like) film modified electrodes: Application to metal cations electroanalysis, Electrochim. Acta 52 (2007) 3082–3087.
[18] V.N. Kislenko, L.P. Oliynyk, Complex formation of polyethyleneimine with copper(II), nickel(II), and cobalt(II) ions, J. Polym. Sci. Part A: Polym. Chem. 40 (2002) 914–922.
[19] M. Amara, H. Kerdjoudj, Modification of the cation exchange resin properties by impregnation in polyethyleneimine solutions: application to the separation of metallic ions, Talanta 60 (2003) 991–1001.
[20] Z.Q. Yuan, Y. Du, Y. He, S.Y. Edward, Sensitive and Selective Detection of Copper Ions with Highly Stable Polyethyleneimine-Protected Silver Nanoclusters, Anal. Chem. 86 (2014) 419–426.
[21] B.L. Johan, L. Mikae, R.C. Bryan, M.S. William, N. Magnus, Polyethyleneimine for copper absorption: kinetics, selectivity and efficiency in artificial seawater, RSC Adv. 4 (2014) 25063–25066.
[22] D.P. Sui, H.T. Fan, J. Li, Y. Li, Q. Li, T. Sun, Application of poly (ethyleneimine) solution as a binding agent in DGT technique for measurement of heavy metals in water, Talanta 114 (2013) 276–282.
[23] F.L. Pissetti, I.V.R. Yoshida, Y. Gushikem, Y.V. Kholin, Metal ions adsorption from ethanol solutions on ethylenediamine-group modified poly (dimethylsiloxane) elastomeric network, Colloid Surf. A-Physicochem. Eng. Asp. 328 (2008) 21–27.
[24] C.H. Xiong, X.Y. Chen, X.Z. Liu, Characterization and application of ethylenediamine-group functionalized chelating resin for copper preconcentration in tea samples, Chem. Eng. J. 203 (2012) 115–122.
[25] W. Li, F. Xia, J. Qu, P. Li, D.H. Chen, Z. Chen, Y. Yu, Y. Lu, R.A. Caruso, W.G. Song, Versatile inorganic-organic hybrid WOx-ethylenediamine-group nanowires: Synthesis, mechanism and application in heavy metal ion adsorption and catalysis, Nano Res 7 (2014) 903–916.

[26] M.Q. Li, J. Wu, L. Cui, H.X. Ju, Selective and sensitive electrochemical determination of Pb^{2+} based on highly adsorptive WOx-ethylenediamine-group nanowires, J. Electroanal. Chem. 757 (2015) 23–28.
[27] I.W. Mwangi, J.C. Ngila, Removal of heavy metals from contaminated water using ethylenediamine-group-modified green seaweed (Caulerpa serrulata), Phys. Chem. Earth. 50–52 (2012) 111–120.
[28] H. Yu, F.T. Zi, X.Z. Hu, J. Zhong, Y.H. Nie, P.Z. Xiang, The copper–ethanediamine-group–thiosulphate leaching of gold ore containing limonite with cetyltrimethyl ammonium bromide as the synergist, Hydrometallurgy 150 (2014) 178–183.
[29] S. Chella, K. Pratap, F. Sathiyanathan, V. Venugopal, K.J. Soon, N.G. Andrews, CoFe2O4 and NiFe2O4@graphene adsorbents for heavy metal ions–kinetic and thermodynamic analysis, RSC Adv. 5 (2015) 28965–28972.
[30] L.C. Zhou, L.Q. Ji, P.C. Ma, Y.M. Shao, H. Zhang, W.J. Gao, Y.F. Li, Development of carbon nanotubes-$CoFe_2O_4$ magnetic hybrid material for removal of tetrabromobisphenol A and Pb(II), J. Hazard. Mater. 265 (2014) 104–114.
[31] Z.C. Ma, D.Y. Zhao, Y.F. Chang, S.T. Xing, Y.S. Wu, Y.Z. Gao, Synthesis of MnFe2O4@Mn–Co oxide core–shell nanoparticles and their excellent performance for heavy metal removal, Dalton Trans. 42 (2013) 14261–14267.
[32] W. Jiang, W.F. Wang, B.C. Pan, Q.X. Zhang, W.M. Zhang, L. Lv, Facile Fabrication of Magnetic Chitosan Beads of Fast Kinetics and High Capacity for Copper Removal, ACS Appl. Mater. Interfaces 6 (2014) 3421–3426.
[33] S.Q. Xiong, B.Y. Yang, D.Q. Cai, G.N. Qiu, Z.Y. Wu, Individual and Simultaneous Stripping Voltammetric and Mutual Interference Analysis of Cd^{2+}, Pb^{2+} and Hg^{2+} with Reduced Graphene Oxide-Fe_3O_4 Nanocomposites, Electrochim. Acta 185 (2015) 52–61.
[34] Y.W. Zhu, S. Murali, M.D. Stoller, K.J. Ganesh, W.W. Cai, P.J. Ferreira, A. Pirkle, R. M. Wallace, K.A. Cychosz, M. Thommes, D. Su, E.A. Stach, R.S. Ruoff, Carbon-Based Supercapacitors Produced by Activation of Graphene, Science 332 (2011) 1537–1541.
[35] Y. Wei, R. Yang, Y.X. Zhang, L. Wang, J.H. Liu, X.J. Huang, High adsorptive (-AlOOH(boehmite)@SiO_2/Fe_3O_4 porous magnetic microspheres for detection of toxic metal ions in drinking water, Chem. Commun. 47 (2011) 11062–11064.
[36] Z.Q. Zhao, X. Chen, Q. Yang, J.H. Liu, X.J. Huang, Selective adsorption toward toxic metal ions results in selective response: electrochemical studies on a polypyrrole/reduced graphene oxide nanocomposite, Chem. Commun. 48 (2012) 2180–2182.
[37] Y. Wei, C. Gao, F.L. Meng, H.H. Li, L. Wang, J.H. Liu, X.J. Huang, SnO_2/reduced graphene oxide nanocomposite for the simultaneous electrochemical detection of cadmium(II), lead(II), copper(II), and mercury(II): an interesting favorable mutual interference, J. Phys. Chem. C 116 (2012) 1034–1041.
[38] Z.Q. Zhao, X. Chen, Q. Yang, J.H. Liu, X.J. Huang, Beyond the selective adsorption of polypyrrole-reduced graphene oxide nanocomposite toward Hg^{2+}: Ultra-sensitive and −selective sensing Pb^{2+} by stripping voltammetry, Electrochem. Commun. 23 (2012) 21–24.
[39] R.X. Xu, X.Y. Yu, C. Gao, J.H. Liu, R.G. Compton, X.J. Huang, Enhancing selectivity in stripping voltammetry by different adsorption behaviors: the use of nanostructured Mg-Al-layered double hydroxides to detect Cd(II), Analyst 138 (2013) 1812–1818.
[40] Y.J. Yao, Z.H. Yang, D.W. Zhang, W.C. Peng, H.Q. Sun, S.B. Wang, Magnetic $CoFe_2O_4$-Graphene Hybrids: Facile Synthesis, Characterization, and Catalytic Properties, Ind Eng. Chem. Res. 51 (2012) 6044–6051.
[41] L.Y. Wang, J. Bao, L. Wang, F. Zhang, Y.D. Li, One-Pot Synthesis and Bioapplication of Amine-Functionalized Magnetite Nanoparticles and Hollow Nanospheres, Chem. Eur. J. 12 (2006) 6341–6347.
[42] L.C. Tan, Q. Liu, D.L. Song, X.Y. Jing, J.Y. Liu, R.M. Li, S.X. Hu, L.H. Liu, J. Wang, Uranium extraction using a magnetic $CoFe_2O_4$-graphene nanocomposite: kinetics and thermodynamics studies, New J. Chem. 39 (2015) 2832–2838.
[43] L.J. Xu, W. Chu, L. Gan, Environmental application of graphene-based $CoFe_2O_4$ as an activator of peroxymonosulfate for the degradation of a plasticizer, Chem. Eng. J. 263 (2015) 435–443.
[44] M.Y. Liu, J.Z. Ji, X.Y. Zhang, X.Q. Zhang, B. Yang, F.J. Deng, Z. Li, K. Wang, Y. Yang, Y. Wei, Self-polymerization of dopamine-group and polyethyleneimine: novel fluorescent organic nanoprobes for biological imaging applications, J. Mater. Chem. B 3 (2015) 3476–3482.
[45] S. Maya, M. Giridhar, B. Suryasarathi, Contrasting Effects of Graphene Oxide and Poly(ethylenimine) on the Polymorphism in Poly(vinylidene fluoride), Cryst. Growth Des. 15 (2015) 3345–3355.
[46] F.X. Qie, G.X. Zhang, J.X. Hou, X.M. Sun, S.Z. Luo, T.W. Tan, Nucleic acid from beans extracted by ethanediamine-group magnetic particles, J Food Sci. Technol. 52 (2015) 1784–1789.
[47] W. Jiang, W.F. Wang, B.C. Pan, Q.X. Zhang, W.M. Zhang, L. Lv, Facile Fabrication of Magnetic Chitosan Beads of Fast Kinetics and High Capacity for Copper Removal, ACS Appl. Mater. Interfaces 6 (2014) 3421–3426.
[48] W. Li, F. Xia, J. Qu, P. Li, D.H. Chen, Z. Chen, Y. Yu, Y. Lu, R.A. Caruso, W.G. Song, Versatile inorganic-organic hybrid WOx-ethylenediamine nanowires: Synthesis, mechanism and application in heavy metal ion adsorption and catalysis, Nano Res. 7 (2014) 903–916.
[49] M.M. Alaie, M. Jahangiri, A.M. Rashidi, A.H. Asl, N. Izadi, A novel selective H_2S sensor using dodecylamine and ethylenediamine functionalized graphene oxide, J. Ind. Eng. Chem. 29 (2015) 97–103.
[50] Y.C. Dong, Y.S. Chui, R.G. Ma, C.W. Cao, H. Cheng, Y.Y. Li, J.A. Zapien, One-pot scalable synthesis of Cu-$CuFe_2O_4$/graphene composites as anode materials for lithium-ion batteries with enhanced lithium storage properties, J. Mater. Chem. A 2 (2014) 13892–13897.
[51] R.S. Freire, L.T. Kubota, Application of self-assembled monolayer-based electrode for voltammetric determination of copper, Electrochim. Acta 49 (2004) 3795–3800.
[52] W.R. Yang, J.J. Gooding, D.B. Hibbert, Characterisation of gold electrodes modified with self-assembled monolayers of L-cysteine for the adsorptive stripping analysis of copper, J. Electroanal. Chem. 516 (2001) 10–16.
[53] D.W.M. Arrigan, L.L. Bihan, A study of L-cysteine adsorption on gold via electrochemical desorption and copper(II) ion complexation, Analyst 124 (1999) 1645–1649.
[54] G.D. Liu, Y.Y. Lin, H. Wu, Y.H. Lin, Voltammetric Detection of Cr(VI) with Disposable Screen-Printed Electrode Modified with Gold Nanoparticles, Environ. Sci. Technol. 41 (2007) 8129–8134.
[55] M. Lin, X.K. Hu, Z.H. Ma, L.X. Chen, Functionalized polypyrrole nanotube arrays as electrochemical biosensor for the determination of copper ions, Anal. Chim. Acta 746 (2012) 63–69.
[56] D.F. Wang, Y.C. Ke, D. Guo, H.G. Guo, J.H. Chen, W. Weng, Facile fabrication of cauliflower-like MIL-100(Cr) and its simultaneous determination of Cd^{2+}, Pb^{2+}, Cu^{2+} and Hg^{2+} from aqueous solution, Sens. Actuator b-Chem. 216 (2015) 504–510.
[57] W. Song, L. Zhang, L. Shi, D.W. Li, Y. Li, Y.T. Long, Simultaneous determination of cadmium(II), lead(II) and copper(II) by using a screen-printed electrode modified with mercury nano-droplets, Microchim Acta 169 (2010) 321–326.
[58] X.X. Xu, G.T. Duan, Y. Li, G.Q. Liu, J.J. Wang, H.W. Zhang, Z.F. Dai, W.P. Cai, Fabrication of gold nanoparticles by laser ablation in liquid and their application for simultaneous electrochemical detection of Cd^{2+}, Pb^{2+}, Cu^{2+}, Hg^{2+}, ACS Appl. Mater. Interfaces 6 (2014) 65–71.